

Topology Simplification for Turbulent Flow Visualization

Xavier Tricoche

University of Kaiserslautern
Department of Computer Science, Computer Graphics & CAGD
P.O. Box 3049, D-67653 Kaiserslautern
Germany
E-mail: tricoche@informatik.uni-kl.de

Abstract

Topology-based methods have become standard tools for the visualization of planar vector and tensor fields. This success is due to their ability to convey huge discrete datasets into synthetic graph depictions that exhibit all qualitative properties of the flow. In that way one reduces dramatically the amount of information while preserving insight into essential characteristics. Yet, in the case of turbulent flows the original technique of topology visualization leads to cluttered images and inconveniences interpretation. The paper presents a continuous topology simplification method that attack this deficiency. It works for vector and tensor fields. Its basic principle is to identify unimportant features in the original graph before modifying the field in a neighborhood to force their pruning. The deformation ensures structural consistency with the original topology. The theoretical background is given by the theory of bifurcations that permits an interpretation of this transformation as a continuous process.

1 Introduction

Vector and tensor visualization is an issue of major interest for many scientific and engineering areas. Namely these mathematical objects play a key role in the qualitative and quantitative description of numerous phenomena like e.g. in fluid dynamics, solid mechanics, magnetics but also computational fluid dynamics (CFD) or finite element analysis. Today's numerical simulations or experimental measurements provide scientists and engineers with huge amount of vector and tensor data that must be analyzed and interpreted. Therefore there is a need for visualization techniques that convey this discrete, abstract input data into meaningful pictures that permit to extract efficiently the essential information. In this context topology-based visualization methods have proved very successful in enabling a good insight into the qualitative nature of vector and tensor field while dramatically reducing the size of the data required for analysis. They were initially designed for vector fields [5, 6, 7] before being extended to symmetric, second-order tensor fields [9, 10]. Their inspiration leads back to the qualitative theory of dynamical systems [1, 2] on one hand and differential geometry [3] on the other hand. Their basic principle consists in focusing the visualization of the field on its singularities and on special integral curves that connect them, partitioning the domain into subregions of uniform qualitative behavior. This results in a synthetic graph depiction that points out the features of major interest for the identification of both local and global flow properties. Yet turbulent flows, like those typically encountered in CFD simulations, are usually associated with vector and tensor topologies characterized by the presence of many structures of very small scale. Their proximity and interconnection in the global depiction result in visual clutter with classical methods. Moreover, this drawback is emphasized by low-order interpolation schemes, typically used

in practice (like linear or bilinear interpolation), because they lack the local flexibility required to precisely reproduce close topological features. Consequently they confuse the results by introducing artifacts. For these reasons topology-based methods produce in this context pictures that inconvenience analysis because essential features cannot be distinguished from local details or numerical noise.

These deficiencies explain why a simplification method is required to prune insignificant features according to qualitative and quantitative criteria, specific to the considered application. The problem was first addressed by de Leeuw et al. [11]. Their method removes pairs of singular points connected by the topological graph along with the corresponding edges while preserving consistency with the original topology. The method is graph-based and ignores the underlying continuous data. Hence, no description of the vector field is provided that corresponds to the simplified topology: Other classical flow visualization methods, e.g. streamlines or LIC [8], cannot be applied afterward to offer consistent depictions. In previous work [12, 13] we proposed an alternative approach for vector and tensor fields in which close singularities are merged, resulting in a higher order singularity that synthesizes the structural impact of several features of small scale in the large. This reduces the number of singularities as well as the global complexity of the graph. Nevertheless this technique has several limitations: First, it implies local grid deformations to simulate the singularities' merging combined with local modifications of the interpolation scheme. Second, it is unable to remove completely singular points due to numerical noise since a singularity is always introduced afterwards. At last, the simplification can only be conducted with respect to geometric criteria (the relative distance of neighboring singularities) which can lead to the disappearance of meaningful flow features.

The new method presented next has been designed to overcome these drawbacks and to offer a continuous way to simplify the topology of planar vector and symmetric, second-order tensor fields. The basic idea consists in successively removing pairs of singularities from the graph while preserving the consistency of the field structure. Each of these removals is induced by a forced local deformation that brings a part of the topology to a simpler, equivalent, uniform structure. The mathematical foundation of these deformations is given by the theory of bifurcations (see e.g. [4]). Practically, the method starts with a planar piecewise linear triangulation. We first compute the topology and associate singularities' pairs with numerical measures that evaluate their relevancy in the global structure. Next, we sort the pairs according to these criteria and retain those with values over prespecified thresholds. Then we process all pairs sequentially. For each of them we first determine a cell pad enclosing both singular points. In this pad, we slightly modify the field values such that the singular points disappear. This deformation is controlled by angular constraints on the new values imposed by those kept constant on the frame of the pad. The processing ends with the recomputation of the simplified topology.

The contents are structured as follows. We review basic notions of vector and tensor field topology and briefly consider a special type of local bifurcation in section 2. The strategy used to determine the significance of singularities' pairs and sort them for removal is discussed in section 3. Section 4 details how local deformations of the field are carried out to suppress the selected pairs. Results are finally proposed on a vector and a tensor CFD dataset in section 5.

2 Topology

For visualization purposes the topology of a vector or a tensor field is the qualitative structure of the associated flow. This flow is defined as the set of all tangential curves integrated in the field, stream lines or tensor lines. Of particular interest are the locations where these curves do not behave uniformly. They correspond to so-called singularities and constitute the nodes of the topological graph. In their neighborhood few curves play a special role. Integrated away from the singular point they build the edges of the topology. This definition is completed by adding closed orbits. Further, essential qualitative properties of a field can be characterized thanks to the notion of index. Precise definitions are given next.

2.1 Vector Field Topology

The singular points (or *critical points*) of a vector field are the positions where the field magnitude vanishes. Their specificity is the fact that they are the only locations where stream lines can meet. The classification of critical points is based in the linear case (sufficient for the present method) on the eigenvalues of the Jacobian matrix. Depending on the real and imaginary parts of these eigenvalues there exist several basic configurations shown in Fig. 1.

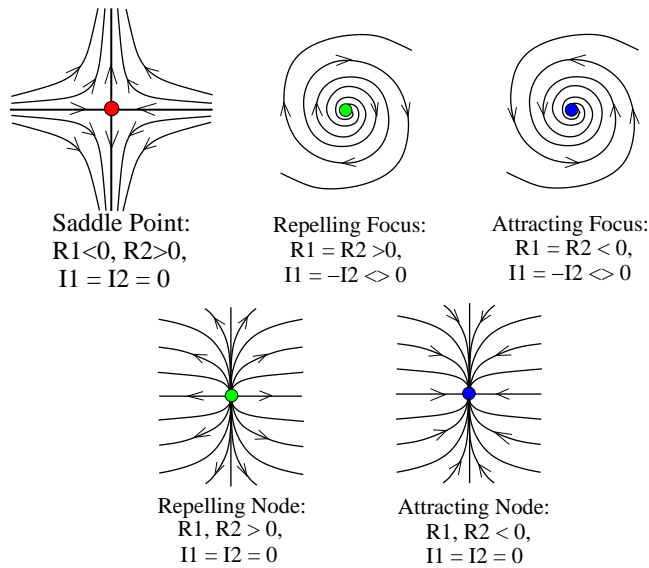


Figure 1: Basic configurations of 1st-order critical points

The separatrices mentioned above are the curves connected to saddle points along the eigenvectors. For every other type of critical point the sign of both eigenvalues' real parts is either positive or negative, corresponding to a repelling (source) or an attracting (sink) nature respectively. Hence a separatrix is linked to a saddle point and typically starts at a source or ends at a sink. Some additional topological features play the role of source or sink in a vector field: These are closed orbits that are also limit cycles

because of the asymptotic behavior of the streamlines in their vicinity. Fig. 2 illustrates such a configuration. These streamlines are periodic.

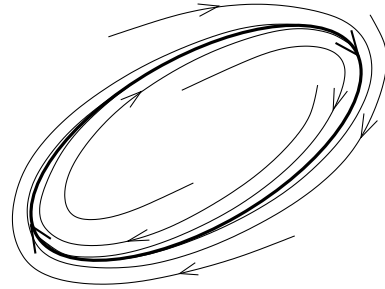


Figure 2: Attracting closed orbit (sink)

A fundamental concept in vector field topology is the so-called Poincaré index (or simply index) of a simple closed curve: It measures the number of rotations of the vector field while traveling once along the curve in positive direction. Remind that the index is always an integer by continuity of the field. By extension one defines the index of a critical point as the index of a simple closed curve around its position. Dealing with first-order critical points saddles have index -1 whereas sources and sinks have index +1. Furthermore the index of a closed orbit is +1. In the following we will make use of two fundamental properties: First, the index of a region enclosing no critical point is zero. Second, the index of a region enclosing several critical points is the sum of their individual indices. Now in linear vector fields there is at most one single critical point (except in degenerate cases). Moreover this critical point has either index +1 or -1. Hence if the index of a closed curve is zero it contains no critical point.

2.2 Tensor Field Topology

Two-dimensional symmetric second-order tensors are in fact 2×2 symmetric matrices. A real two-dimensional symmetric matrix M has always two (not necessarily distinct) real eigenvalues $\lambda_1 \leq \lambda_2$ with associated orthogonal eigenvectors. Per definition, eigenvectors have neither norm nor orientation which distinguishes them fundamentally from the classical vectors considered previously. Since the computation of the eigenvectors of M is not affected by the isotropic part (which is multiple of the identity matrix) we only consider the trace-free part of M , called deviator. Thus we process in the tensor case matrix-valued functions of the form:

$$T : (x, y) \in U \subset \mathbb{R}^2 \mapsto T(x, y) = \begin{pmatrix} \alpha(x, y) & \beta(x, y) \\ \beta(x, y) & -\alpha(x, y) \end{pmatrix},$$

where α and β are two scalar functions defined over the considered two-dimensional domain. One defines a major (resp. minor) *eigenvector field* at each position of the domain as the eigenvector related to the major (resp. minor) eigenvalue of the tensor field. One defines major (resp. minor) *tensor lines* as the curves everywhere tangent to the major (resp. minor) eigenvector field. Consequently, as opposed to stream lines these curves have no inherent orientation. Yet this definition only holds outside locations where both eigenvalues are equal. There eigenvectors cannot be uniquely determined since every non-zero vector is an eigenvector. These singular points are called degenerate points. They correspond to a zero value of the deviator. Remark that the lack of orientation leads to topological structures unknown

in vector fields. In the linear case these singularities exist in two possible types: *Trisector* or *wedge point* (see Fig. 3). Separatrices

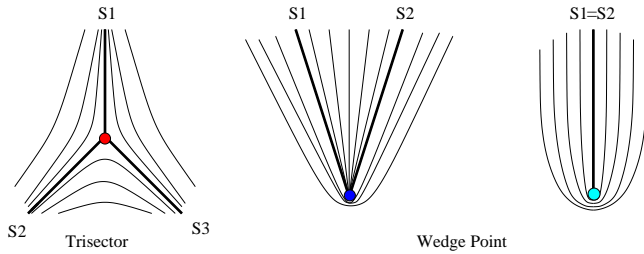


Figure 3: First Order Degenerate Points

emanate here from both wedges and trisectors. They are the curves that bound regions where tensor lines pass by the singularity in both directions, called hyperbolic sectors. Closed tensor lines exist for tensor fields too. Nevertheless they are rare in practice.

The notion of index can be extended in this context. Analogous to the vector case one defines the index of a closed curve as the number of rotations of the eigenvectors along the curve. Since these eigenvectors are orthogonal the tensor index applies to both eigenvector fields. The lack of orientation entails index values multiple of $\frac{1}{2}$. In particular a trisector has index $-\frac{1}{2}$, a wedge has index $+\frac{1}{2}$. An illustration is proposed in Fig. 4. Remark that the properties

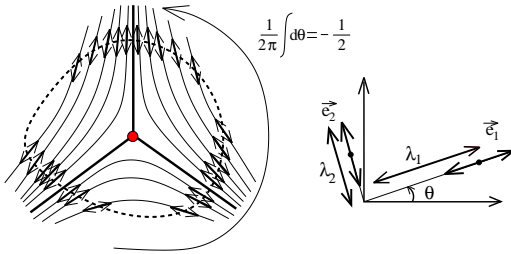


Figure 4: Tensor index of a trisector

mentioned for the vector index hold for the tensor index too.

2.3 Pairwise Annihilations

The definitions introduced previously apply to an instantaneous topological state of a vector or tensor field. Now this stable state may evolve in another one by slight changes of underlying parameters. A typical example is provided by time-dependent fields, the singularities of which may move, appear or vanish over time, leading to topological changes. These changes preserve structural consistency. In particular the index of the concerned region acts as an invariant. If a topological transition only affects a small region of the field it is called *local bifurcation*. If it leads to a global structural change on the contrary this is a *global bifurcation*. For our purpose we only consider a particular kind of local bifurcation: It consists of the pairwise annihilation of two singularities with opposite indices. Since these singularities have global index 0 they are equivalent to a configuration without singular point. Consequently they vanish after merging. The vector case is illustrated in Fig. 5: A saddle point and a sink (resp. source) node are merged. As far as degenerate points are concerned, the situation is shown in Fig. 6. Here a trisector is merged with a wedge.

Practically we want to reduce the number of singularities and associated separatrices while remaining consistent with the original

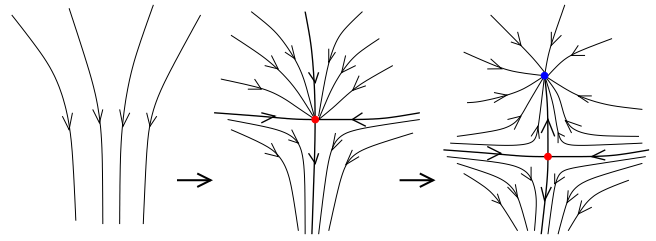


Figure 5: Saddle-node bifurcation

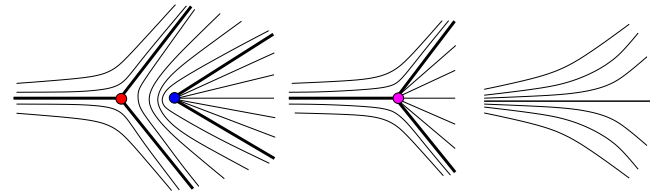


Figure 6: Pairwise annihilation (tensor)

topology. So we force locally pairwise annihilations of a saddle with a node, resp. of a trisector with a wedge. This can be achieved by small local changes in the field values as we show in the following.

3 Selective Pairing of Singularities

As said previously, we aim at annihilating pairs of singular points with opposite indices. Moreover, the corresponding topology simplification must take geometric and any additional criteria into account to fit the considered interpretation of the vector or tensor field. Our geometric criterion is the proximity of the singularities to be removed pairwise. This choice is motivated by two major reasons. First, close singularities result in small features that clutter the global topology depiction since they can hardly be differentiated and induce many separatrices. Second, piecewise linear interpolation is likely to produce topological artifacts consisting of numerous close first-order singularities, especially if numerical noise is an issue. Therefore, given a proximity threshold, we determine all possible pairs of saddle and sinks, resp. wedges and trisectors, satisfying the geometric criterion and sort them in increasing distance. Remark that in the vector case we only consider pairs of critical points linked by a separatrix which strongly restricts the range of possible pairs. Unfortunately this criterion cannot be applied to tensor topologies since every degenerate point exhibits at least one hyperbolic region. This entails that separatrices emanating from a singularity often do not reach any other one, i.e. separatrices often leave the domain through the boundary. Additional criteria may be introduced to restrict the range of the considered singularities to those that are little relevant for interpretation. Basically a quantity is provided that characterizes the significance of each singular point and one retains for simplification only those with a value under a user-prescribed threshold. Consequently if a given singularity is considered important for interpretation it will be left apart. Doing so it will not be removed from the topology.

Practically we will consider in section 5 the norm of the including cell as a criterion to characterize the importance of a critical point. As a matter of fact singularities located in a cell with tiny vector field magnitude are likely to be due to numerical noise.

4 Local Deformation

Once a pair of singularities has been identified that fulfills our criteria it must be removed. To do this we start a local deformation of the field in a small area around the considered singular points. Practically we only modify vector or tensor values at the vertices of the triangulation and do not change the interpolation scheme. This ensures obviously continuity over the grid after modification. In the following we detail first how vertices to be modified are determined. Next we explain how new values are set at those vertices to ensure the absence of remaining singular points in their incident cells afterwards.

4.1 Cell-wise Connection

Consider the situation shown in Fig. 7. We first compute the intersections of the straight line connecting the first singular point to the second with the edges of the triangulation. For each intersection point, we insert the grid vertex closest to the second singular point (see vertices surrounded by a circle) in a temporary list. After this, we compute the bounding box of all vertices in the list and include all grid vertices contained in this box. This includes every vertex marked in the former step. The vertices concerned with modifica-

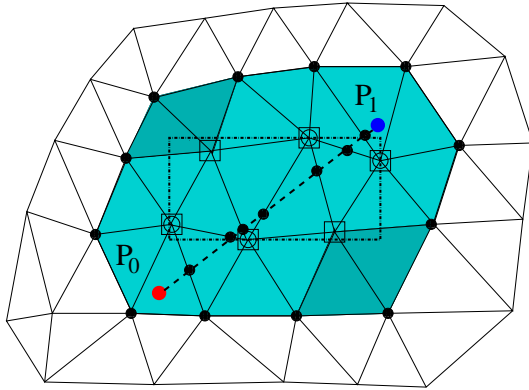


Figure 7: Cell-wise connection

tion are surrounded by squares. We call them *internal vertices* in the following. Since the modification of a vertex value has an incidence on the topology in all triangle cells it belongs to we include every cell incident to a selected vertex in the cell group. These cells are colored gray. Further processing will have to associate the internal vertices with values that ensure the absence of any singular point in the cell group with respect to the values defined at the *boundary vertices* (marked by big dots in Fig. 7) that will not be changed. Notice that the connection fails if one of the included cells contains a singular point that does not belong to the current pair. In this case the global index of the cell group is no longer zero. If it occurs we interrupt the processing of this pair. Nevertheless such cases can be mostly avoided by simplifying pairs of increasing distance.

4.2 Angular Constraints

The basic principle of the local simplification technique is better understood when considering a single internal vertex together with its incident triangles: See Fig. 8. Suppose that every position marked black is associated with a constant value and the global index of the triangle stencil is zero. The problem consists in determining a new tensor value at the internal vertex (in white) such that no incident

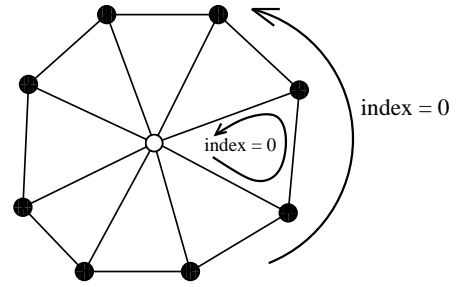


Figure 8: Configuration with single intern vertex and incident cells

cell contains a critical point. This is equivalent to a situation where every incident triangle has index 0 according to what precedes.

We come now to an important property of linear vector and tensor fields that is used to drive the pairwise removal of singularities.

Property 4.1 *The angle variation of a linear vector field (resp. eigenvector field of a linear tensor field) along an edge is always smaller than π (resp. $\frac{\pi}{2}$).*

This is obvious in the vector case. For a proof in the tensor case see [15]. We now use this property to compute the index of a linear vector (resp. tensor) field along the edges of a triangle. Since the field is linear it is determined by the three values at the vertices of the triangle. We denote $\theta_0, \theta_1, \theta_2$ the corresponding angle coordinates of the vectors (resp. eigenvectors) enumerated in counterclockwise order. Because eigenvectors have no orientation the angles are in this case defined modulo π . We set by convention $\theta_3 := \theta_0$, so we have

$$\text{index} = \sum_{i=0}^2 \Delta(\theta_i, \theta_{i+1}). \quad (1)$$

To unify the discussion we introduce the symbol σ that we define as $\sigma := 2\pi$ in the vector case and $\sigma := \pi$ in the tensor case. Furthermore we set $\delta_i := \theta_{i+1} - \theta_i$. With the property above we have finally

$$\Delta(\theta_i, \theta_{i+1}) = \begin{cases} \delta_i & \text{if } |\delta_i| < \frac{\sigma}{2} \\ \delta_i + \sigma & \text{if } \delta_i < -\frac{\sigma}{2} \\ \delta_i - \sigma & \text{if } \delta_i > \frac{\sigma}{2}. \end{cases}$$

Getting back to a given triangle of the stencil depicted above, the angle coordinates of the vectors (resp. eigenvectors) defined at the black vertices (say θ_0 and θ_1) induce an angular constraint for the new value. Indeed in Equation 1 $\Delta(\theta_0, \theta_1)$ is already set to a value that is strictly smaller than $\frac{\sigma}{2}$. The two missing terms must induce a global angle change smaller than σ (for the index of a linear singular point is a multiple of $\frac{\sigma}{2\pi}$). It will be the case if and only if the new vector (resp. eigenvector) value has angle coordinate in $]\theta_1 + \frac{\sigma}{2}, \theta_0 + \frac{\sigma}{2}[$ (modulo σ), with $[\theta_0, \theta_1]$ being an interval with width smaller than $\frac{\sigma}{2}$, i.e. the actual angle change along a linear edge from θ_0 to θ_1 (see Fig. 9).

This provides a angle constraint on the new value for a single triangle. Intersecting the intervals imposed by all incident triangles, one is eventually able to determine an interval that fulfills all the constraints. Notice that this interval may be empty. In this case the simplification is (at least temporarily) impossible. Once a satisfactory angle interval has been found we provide the vertex with a corresponding value. In the vector case, the magnitude is set to the average of the field magnitude on the stencil boundary. In the tensor case if θ is an angle in the interval the following tensor value will be solution:

$$T_{new} = \begin{pmatrix} \cos 2\theta & \sin 2\theta \\ \sin 2\theta & -\cos 2\theta \end{pmatrix}.$$

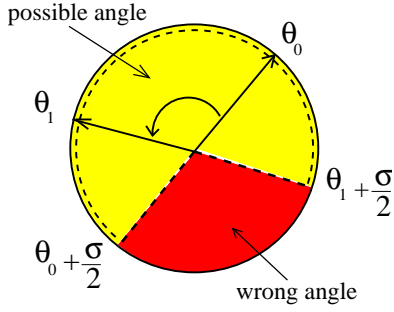


Figure 9: Angular constraint in a triangle cell (modulo σ)

4.3 Iterative Solution

For each internal vertex (see Fig. 7) we must now find a new vector (resp. tensor) value that fulfills all the angle constraints induced by the edges connecting the incident vertices. These incident vertices are of two types: Internal or boundary vertices. Edges linking boundary vertices are considered constant and induce fixed constraints. Internal vertices still must be provided a final value and introduce flexibility in the simplification scheme. The pseudo-code of the method is as follows (mean_angle is the mean value of the neighbors' angles).

```
// initialization
for each (internal vertex)
  interval = fixed constraints
  if (interval is empty)
    interrupt
  end if
  if (no fixed constraints)
    interval = [0, SIGMA[
  end if
end for each

// iterations
nb_iterations = 0
repeat
  succeeded = true
  nb_iterations++
  for each intern vertex
    compute mean_angle of processed incident vertices
    if (interval not empty)
      if (mean_angle in interval)
        current_angle = mean_angle
      else
        current_angle = best approximation
          of mean_angle in interval
      end if
    else
      succeeded = false
      if (mean_angle in fixed constraints)
        current_angle = mean_angle
      else
        current_angle = best approximation
          of mean_angle in interval
      end if
    end for each
  until (succeeded or
    nb_iterations > MAX_NB_ITERATIONS)
```

If one of the internal vertices has incompatible fixed constraints, our scheme cannot succeed. Therefore we interrupt the process during initialization and move to the next pair. If the iterative process failed at determining compatible angular constraints for all internal vertices, we maintain the current pair and move to the next as well.

5 Results

We show the results of the method applied to two datasets stemming from CFD vortex breakdown simulations provided by Wolfgang Kollmann from UC Davis. The first one is a velocity dataset and is of vector type. The second one is a rate of deformation tensor dataset. Both exhibit turbulent behaviors and complex topologies.

5.1 Velocity

The grid is rectilinear and has 124 x 101 vertices ranging from 0 to 9.84 in x and from -3.864 to 3.864 in y . The triangulation has 24600 linearly interpolated cells. The original topology is shown in Fig. 10. There are 94 critical points and 134 corresponding pairs. We first simplify without magnitude control. The only threshold

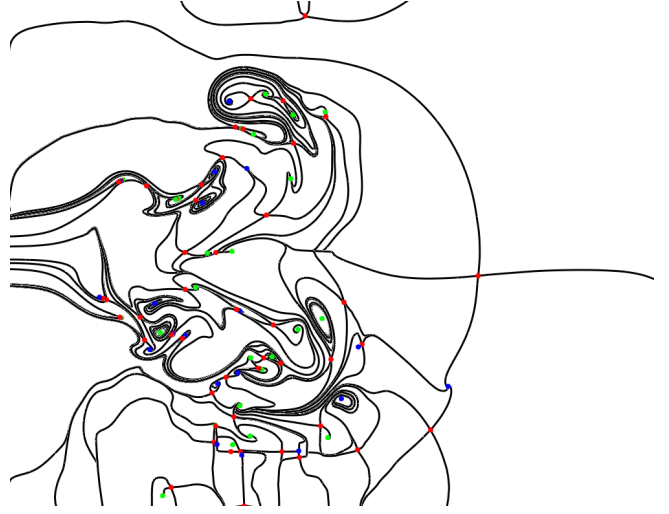


Figure 10: Original vector topology

is therefore the graphical distance between critical points. With a threshold of 1% of the grid width there are 10 removed pairs. With a threshold of 5%, there are 19 removed pairs as shown in Fig. 11. Applying a very large threshold of 50% we obtained the simplified topology shown in Fig. 12. There are only 18 critical points remaining. Focusing on a small part of the topology we observe how features of small scale are removed. Compare Fig. 13(a) and Fig. 13(b).

To show the impact of a norm-based simplification on the topology (i.e. filtering of computational noise) we apply a threshold on the field magnitude and get the results presented in the following table (the threshold is expressed with respect to the largest norm of the vector field).

threshold	satisfying pairs	connected pairs	removed pairs	removed sing.
0.5%	25 (19%)	8 (6%)	8 (6%)	16 (17%)
1%	30 (22%)	11 (8%)	11 (8%)	22 (23%)
5%	47 (35%)	15 (11%)	15 (11%)	30 (32%)
10%	77 (57%)	21 (16%)	21 (16%)	42 (45%)
20%	95 (71%)	28 (21%)	26 (19%)	52 (55%)
50%	115 (86%)	36 (27%)	33 (25%)	66 (70%)

5.2 Rate of Deformation

The topology exhibits 67 singularities and 140 separatrices as shown in Fig. 14 (the picture is rotated for convenience). The rectilinear grid has 123 x 100 cells. Each rectangular cell is split to result in a triangulation containing about 25000 cells. To simplify this



Figure 11: Simplified vector topology: Small graphic threshold (5%)

topology we consider only the euclidean distance between degenerate points as criterion. The first simplified topology is obtained with a tiny distance threshold corresponding to 0.2% of the grid diagonal. Every pair consisting of degeneracies that could not be graphically differentiated has been removed. There are 59 remaining singularities. The modified areas are indicated by rectangular boxes. See Fig. 15. The highest simplification rate is obtained with a threshold of 5% of the grid diagonal. The corresponding topology is proposed in Fig. 16. The fact that this topology cannot be simplified further (even with a very large geometrical threshold) is explained by the presence of incompatible fixed angle constraints on the boundaries of the cell pads containing the remaining pairs. However a noticeably clarified graph can be obtained in this case while global structural properties of tensor field have been preserved. The local deformation corresponding to the simplified topologies shown so far is illustrated in Fig. 17. The topology is displayed together with the underlying cell structure and the eigenvectors.

6 Conclusion

We have presented a method that simplifies the topology of planar vector and symmetric, second-order tensor fields. This post-processing step is necessary for the visualization of turbulent flows like those provided by CFD simulations. Such datasets exhibit very complex structural behaviors. This results in visual clutter and inconveniences interpretation of classical, topology-based depictions. The processing preserves qualitative consistency with the original data. The simplification is achieved by means of successive local deformations of the field that entail the pruning of pairs of singular points with opposite indices. The pairing strategy can take geometrical as well as any additional criterion into account to fit the domain of application. The method makes use of deep connections between vector and eigenvector fields to handle both vector and tensor cases in a very similar way. The mathematical foundation of this technique is provided by the notion of bifurcation. Namely the disappearance of a pair of singularities with opposite indices corresponds to their smooth, pairwise annihilation. The method has been evaluated on both a vector and a tensor CFD dataset stemming from numerical simulations of a vortex breakdown. These datasets exhibit many complex, local features and a complicated global topol-

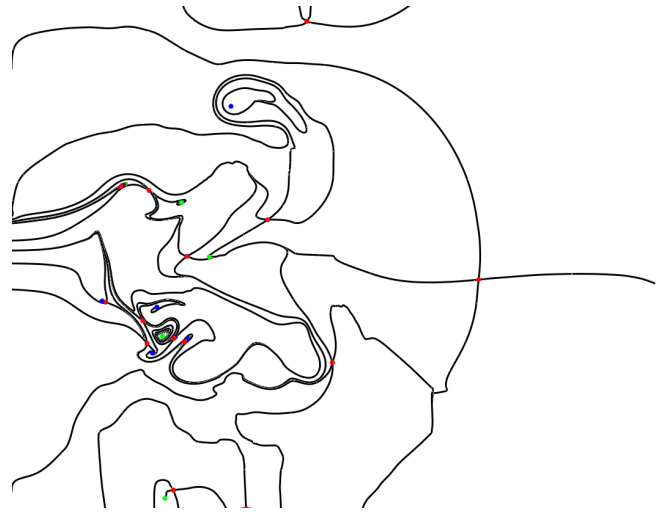


Figure 12: Simplified vector topology: Large graphic threshold (50%)

ogy. The results demonstrate the ability of the method to remove selectively structural features of small scale while letting the rest of the topology unchanged. This clarifies noticeably the depiction and eases interpretation.

References

- [1] H. Poincaré *Sur les courbes définies par une équation différentielle*. J. Math. 1, 1875, pp. 167-244. J. Math. 2, 1876, pp. 151-217. J. Math. 7, 1881, pp. 375-422. J. Math. 8, 1882, pp. 251-296.
- [2] A. A. Andronov, E. A. Leontovich, I. I. Gordon, A. G. Maier, *Qualitative Theory of Second-Order Dynamic Systems*. Israel Program for Scientific Translations, Jerusalem, 1973.
- [3] M. Spivak, *A Comprehensive Introduction to Differential Geometry, Vol. 1-5* Publish or Perish Inc., Berkeley CA, 1979.
- [4] J. Guckenheimer, P. Holmes, *Nonlinear Oscillations, Dynamical Systems and Linear Algebra*. Springer, New York, 1983.
- [5] J. L. Helman, L. Hesselink, *Automated analysis of fluid flow topology*. Three-Dimensional Visualization and Display Technologies, SPIE Proceedings Vol. 1083, 1989, pp. 144-152.
- [6] J. L. Helman, L. Hesselink, *Visualizing Vector Field Topology in Fluid Flows*. IEEE Computer Graphics and Applications, Vol. 11, No. 3, 1991, pp. 36-46.
- [7] A. Globus, C. Levit, T. Lasinski, *A Tool for the Topology of Three-Dimensional Vector Fields*. IEEE Visualization '91 Proceedings, IEEE Computer Society Press, Los Alamitos, 1991, pp. 33-40.
- [8] B. Cabral, L. Leedom, *Imaging Vector Fields Using Line Integral Convolution*. Computer Graphics (SIGGRAPH '93 Proceedings) 27(4), 1993, pp. 263-272.

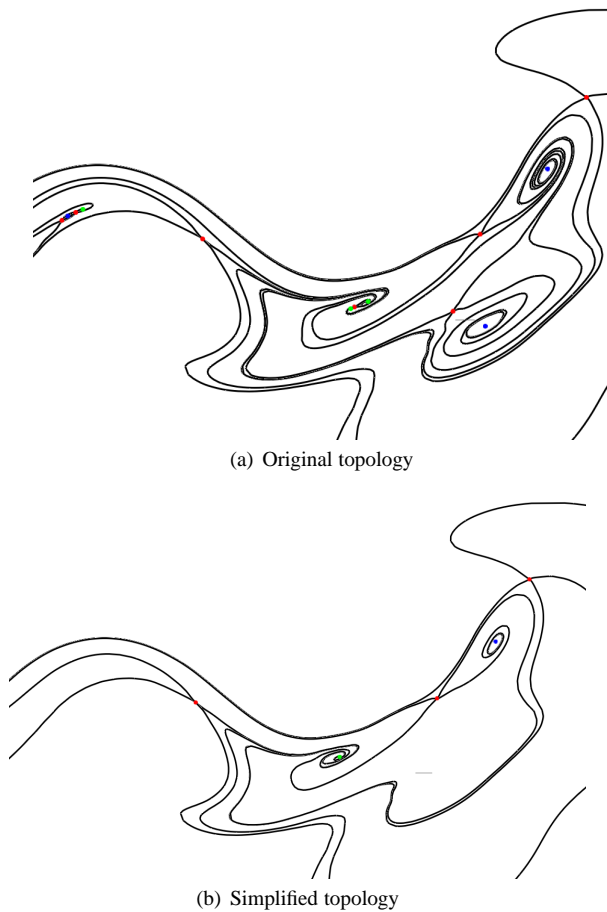


Figure 13: Removal of small scale features (vector)



Figure 14: Initial tensor topology with grid

- [9] T. Delmarcelle, L. Hesselink, *The Topology of Symmetric, Second-Order Tensor Fields*. IEEE Visualization '94 Proceedings, IEEE Computer Society Press, Los Alamitos, 1994, pp. 140-147.
- [10] T. Delmarcelle, *The Visualization of Second-Order Tensor Fields*. PhD Thesis, Stanford University, 1994.
- [11] W. C. de Leeuw, R. van Liere, *Collapsing Flow Topology Using Area Metrics*. IEEE Visualization '99 Proceedings, IEEE Computer Society Press, Los Alamitos, 1999, pp. 349-354.
- [12] X. Tricoche, G. Scheuermann, H. Hagen, *A Topology simplification Method for 2D Vector Fields*. IEEE Visualization '00 Proceedings, IEEE Computer Society Press, Los Alamitos, 2000, pp. 359-366.
- [13] X. Tricoche, G. Scheuermann, H. Hagen, *Vector and Tensor Field Topology Simplification on Irregular Grids*. Proceedings of the Joint Eurographics-IEEE TCVG Symposium on Visualization in Ascona, Switzerland, D. Ebert, J. M. Favre, R. Peikert (eds.), Springer-Verlag, Wien, 2001, pp. 107-116.
- [14] X. Tricoche, G. Scheuermann, H. Hagen, *Continuous Topology Simplification of 2D Vector Fields*. IEEE Visualization '01 Proceedings, IEEE Computer Society Press, Los Alamitos, 2001, pp. 159-166.
- [15] X. Tricoche, *Vector and Tensor Topology Simplification, Tracking, and Visualization*. PhD thesis, Schriftenreihe / Fachbereich Informatik, Universität Kaiserslautern, 3, 2002.

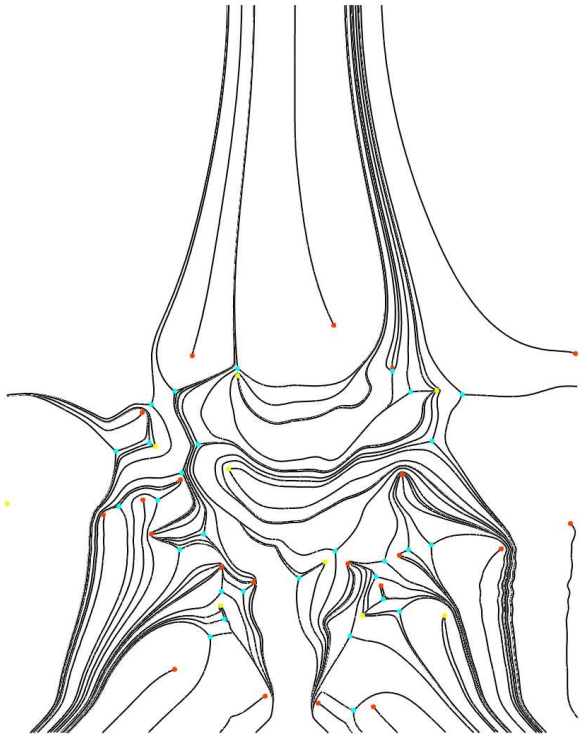


Figure 15: Simplified tensor topology: distance threshold = 0.2%

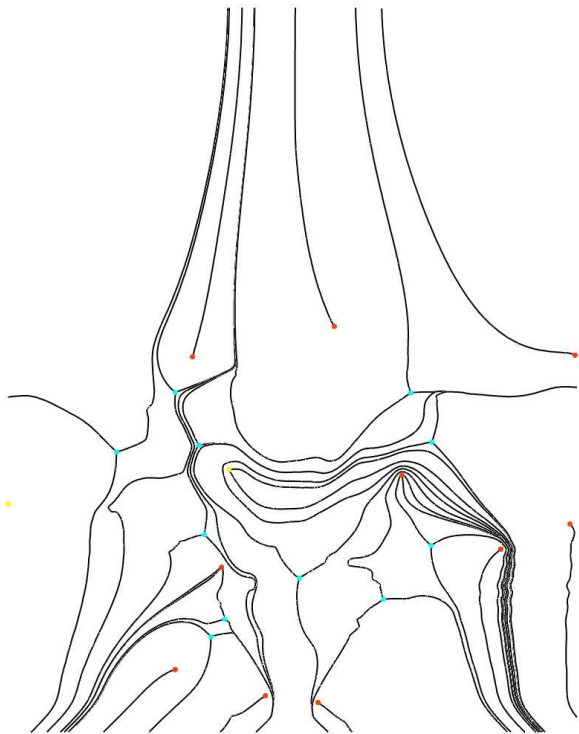


Figure 16: Simplified tensor topology: distance threshold = 5%

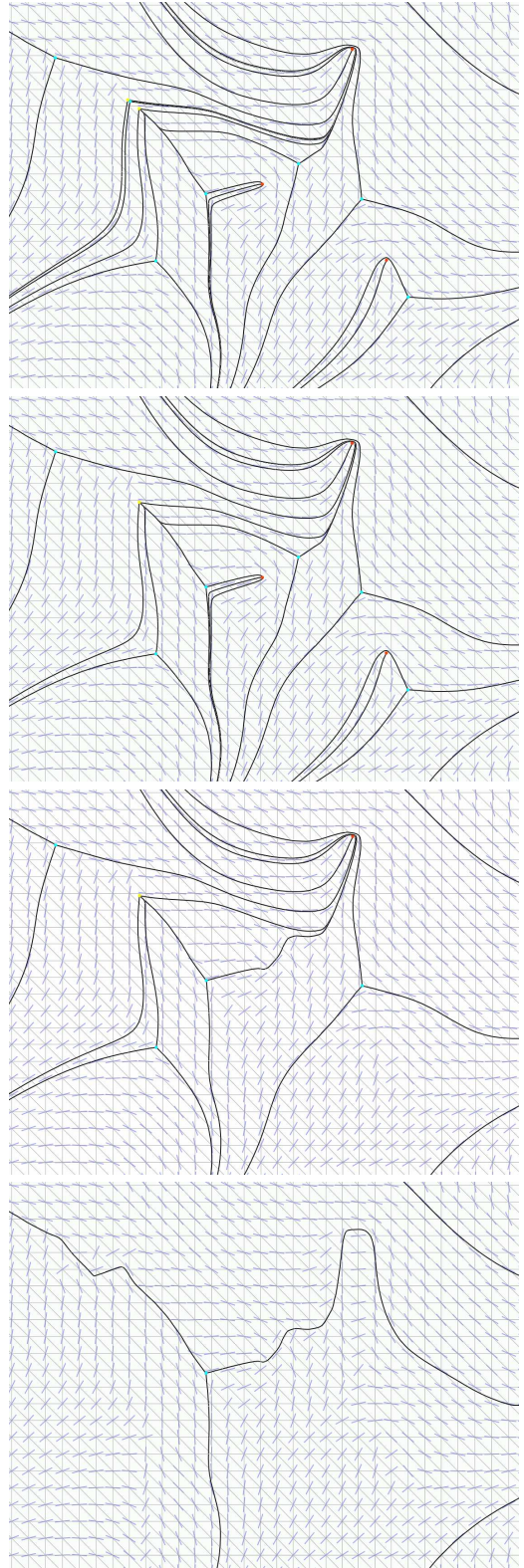


Figure 17: Local topology simplification (tensor): initial graph and simplifications with 0.2%, 2% and 5% as thresholds